

# Supplementary Material

## Resolution model

The root-mean-square of the dimuon mass resolution of simulated  $B^+ \rightarrow K^+ \mu^+ \mu^-$  decays with and without the kinematic fit applied is shown in Fig. 1. The resolution depends strongly on the value of the dimuon mass. The kinematic fit typically improves the resolution by about a factor of two.

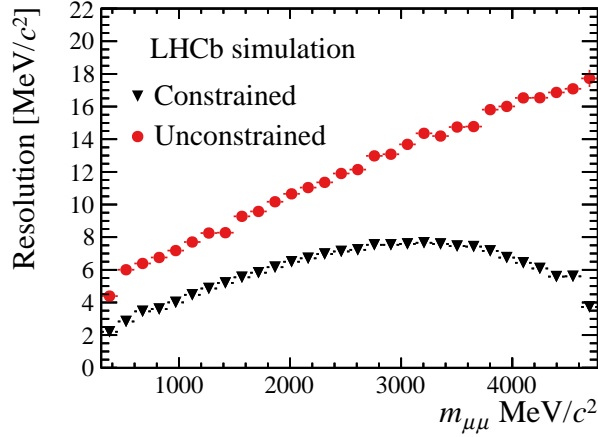


Figure 1: The dimuon mass resolution as a function of  $m_{\mu\mu}$  for simulated  $B^+ \rightarrow K^+ \mu^+ \mu^-$  decays with (black triangles) and without (red circles) the kinematic fit applied.

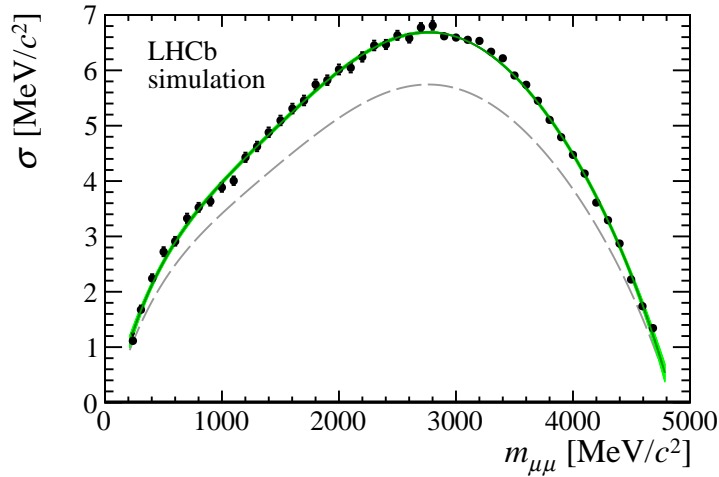


Figure 2: Dependence of the resolution model on  $m_{\mu\mu}$  from simulated events. The width of the Gaussian component,  $\sigma_G$ , is illustrated by the green-solid line and the width of the component with power law tails,  $\sigma_C$ , by the grey-dashed line. The ratio of the two widths is fixed from a large sample of simulated  $B^+ \rightarrow J/\psi K^+$  decays. The data points correspond to the measured value of  $\sigma_G$  for the simulated  $B^+ \rightarrow K^+ \mu^+ \mu^-$  decays.

## Fit result with vector and axial-vector separated

The result of the fit to the data, with vector and axial-vector components separated, is shown below in Fig. 3.

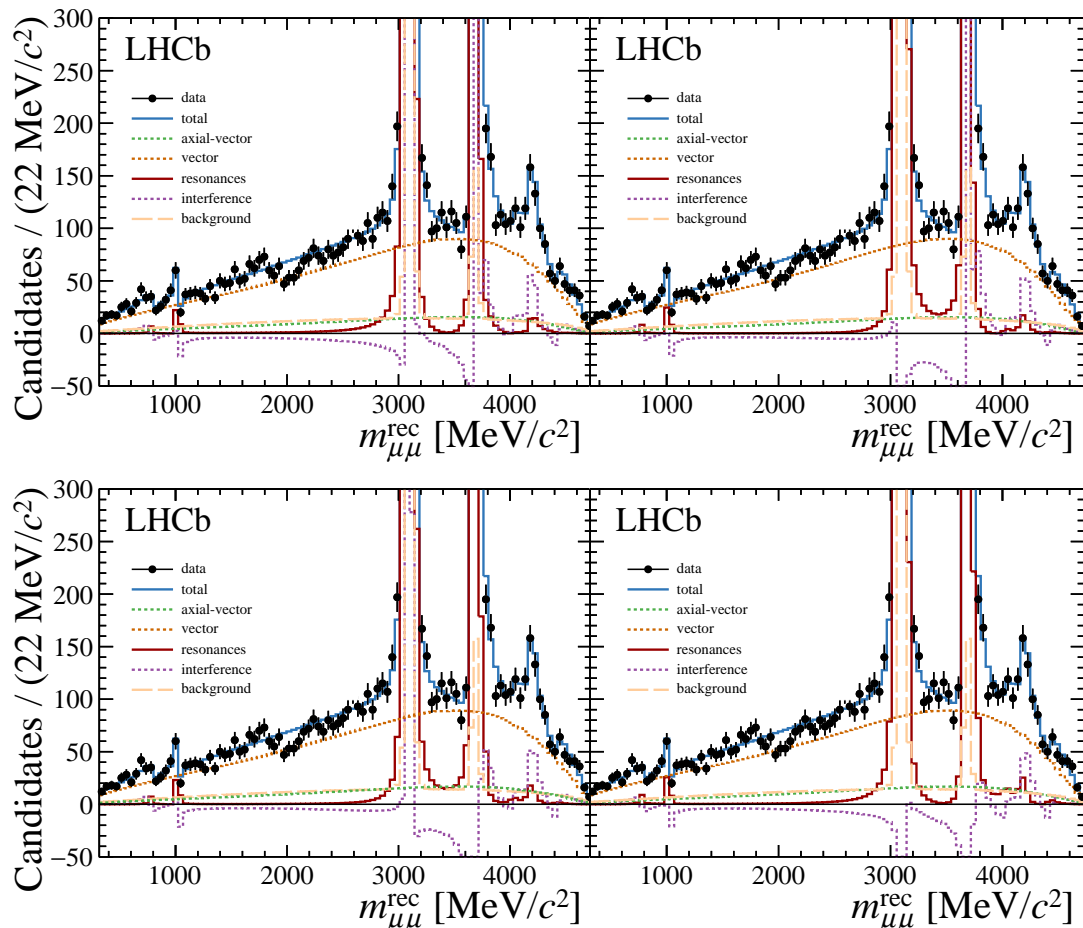


Figure 3: Fits to the dimuon mass distribution for the four different phase combinations that describe the data equally well. In the plots, the  $J/\psi$  and  $\psi(2S)$  phases are both negative (top left); the  $J/\psi$  phase is positive and the  $\psi(2S)$  phase is negative (top right); the  $J/\psi$  phase is negative and the  $\psi(2S)$  phase is positive (bottom left); and both phases positive (bottom right).

## Fit result on a log-scale

The result of the fit to the data, on a log-scale, is shown below in Fig. 4. These fits are identical to the ones in Fig. [3] of the main body of the paper.

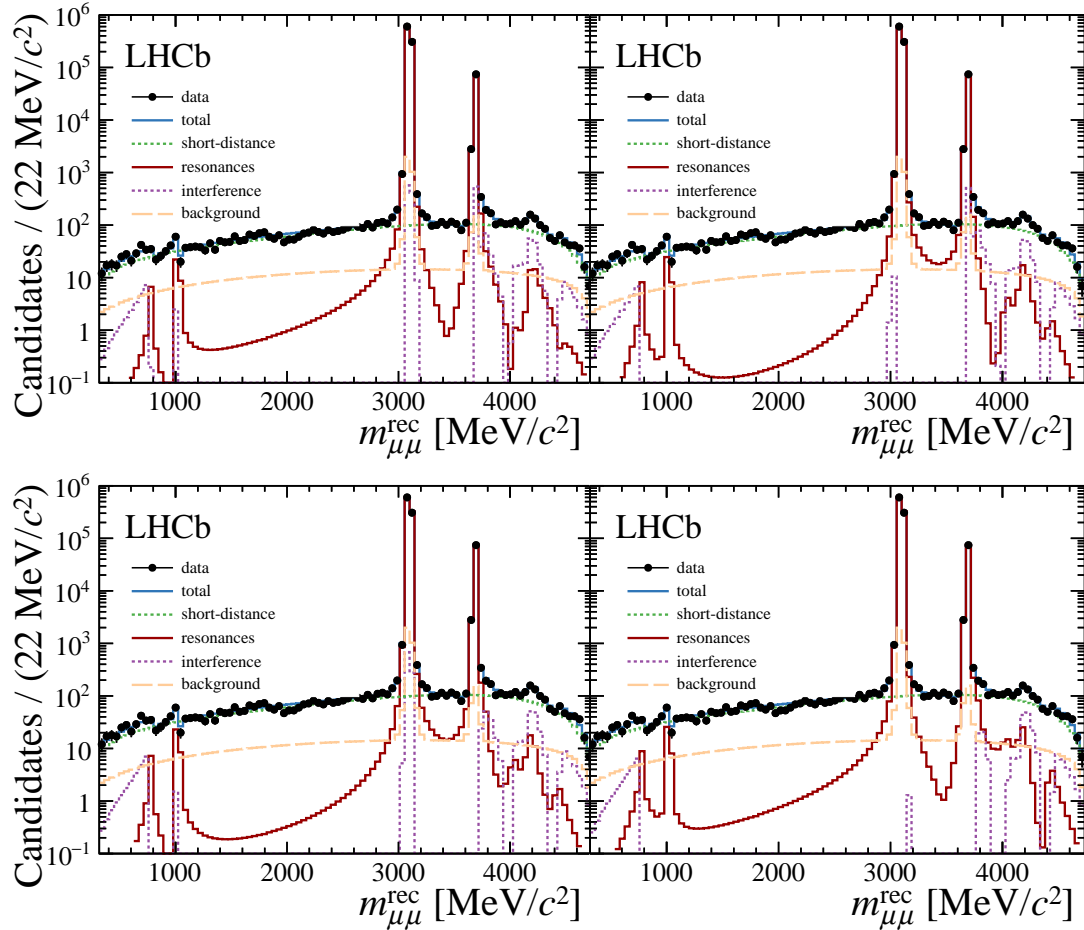


Figure 4: Fits to the dimuon mass distribution for the four different phase combinations that describe the data equally well. In the plots, the  $J/\psi$  and  $\psi(2S)$  phases are both negative (top left); the  $J/\psi$  phase is positive and the  $\psi(2S)$  phase is negative (top right); the  $J/\psi$  phase is negative and the  $\psi(2S)$  phase is positive (bottom left); and both phases positive (bottom right).

## Dependence of the fit on the $J/\psi$ phase

Figure 5 illustrates the sensitivity of the fit to the  $J/\psi$  phase. For simplicity the Wilson coefficients  $\mathcal{C}_7$ ,  $\mathcal{C}_9$  and  $\mathcal{C}_{10}$  are fixed to their SM values and the fit repeated three times. In the first fit the magnitude and phase of all of the resonances are left free. This fit is then repeated fixing the phase of the  $J/\psi$  to be either 0 or  $\pi$  radians.

Note, while the fit quality with  $\mathcal{C}_7$ ,  $\mathcal{C}_9$  and  $\mathcal{C}_{10}$  fixed to their SM values appears good, this fit results in a large pull of the form-factor parameters. This is needed to compensate the values of the Wilson coefficients in explaining the low value of the  $B^+ \rightarrow K^+ \mu^+ \mu^-$  branching fraction.

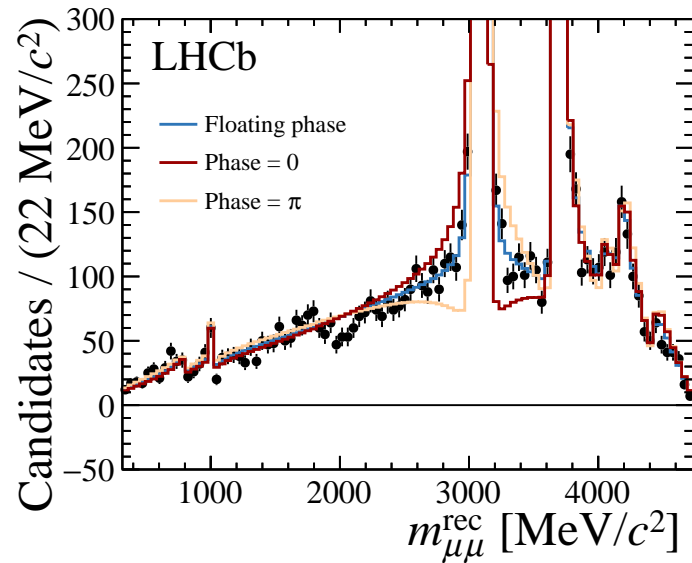


Figure 5: Fits to the dimuon mass distribution with the Wilson coefficients  $\mathcal{C}_7$ ,  $\mathcal{C}_9$  and  $\mathcal{C}_{10}$  fixed to their SM values. The result of three separate fits are shown: one where the phase of the  $J/\psi$  meson is floating, one where it is fixed to zero and one where it is fixed to  $\pi$  radians.